Medium-induced parton splitting kernels from Soft Collinear Effective Theory with Glauber gluons

Grigory Ovanesyan[1] and Ivan Vitev[1]

[1]*Los Alamos National Laboratory, Theoretical Division, MS B238, Los Alamos, NM 87545, USA*

We derive the splitting kernels for partons produced in large Q^2 scattering processes that subsequently traverse a region of strongly-interacting matter using a recently-developed effective theory $\mathrm{SCET_G}$. We include all corrections beyond the small-x approximation, consistent with the power counting of $\mathrm{SCET_G}$. We demonstrate how medium recoil, geometry and expansion scenarios, and phase space cuts can be implemented numerically for phenomenological applications. For the simplified case of infinite transverse momentum kinematics and a uniform medium, we provide closed-form analytic results that can be used to validate the numerical simulations.

I. INTRODUCTION

The suppression in the production rate of energetic leading particles and particle correlations due to final-state interactions in reactions with ultra-relativistic nuclei is among the best-known experimental discoveries at the Relativistic Heavy Ion Collider (RHIC) [1]-[4], and now at the Large Hadron Collider (LHC) [5]-[7]. This jet quenching phenomenon also provides one of the strongest pieces of evidence for the creation of dense strongly-interacting matter in such collisions [8]. Recent advances in understanding the modification of partons and parton showers in Quantum Chromodynamics (QCD) media have come from the inclusion of jets in the theoretical [9]-[16] and experimental [17]-[23] analyses. Jet observables are more sensitive to the underlying theoretical model assumptions and the properties of the QCD medium when compared to leading particle measurements [24].

In recent years effective field theories (EFT) have become a powerful modern tool for jet physics. In particular, Soft Collinear Effective Theory [25–28] (SCET) is an effective theory for QCD that describes the dynamics of highly energetic partons. It has been successfully applied to improve the theoretical accuracy in the evaluation of high energy cross sections at lepton [29]-[32] and hadron colliders [33]-[35].

The first step in constructing an effective theory for jets propagating in a QCD medium was done in Ref. [36], where the SCET Lagrangian was extended by adding a term that describes the interaction of a quark jet with gluons that have momentum purely transverse to it, traditionally referred to in the literature as Glauber gluons. As an application of effective Lagrangian derived in [36], in Ref. [37] the probability density of quark jet broadening [38, 39] was re-derived as an expectation value of Wilson lines, which later the authors evaluate using AdS/CFT correspondence. In Ref. [40] the Yang-Mills part of the collinear SCET Lagrangian was coupled to Glauber gluons, which allowed to perform calculations for parton splitting processes in the medium. The resulting effective theory was called $\mathrm{SCET_G}$, where "G" stands for Glauber gluons. In that paper a detailed connection was made between calculations in $\mathrm{SCET_G}$ and the evaluation of jet broadening [38, 39] and medium-induced quark energy loss in the Gyulassy-Levai-Vitev approach [38, 41]. The gauge invariance of the physics results was explicitly demonstrated for three different gauge choices. One of the medium-induced splittings, namely $q \to qg$ has been calculated in Ref. [40] beyond the soft emitted gluon approximation. There are three additional splittings: $g \to gg, g \to q\bar{q}$ and $q \to gq$. To complete the derivation of all medium-induced branching processes without the assumption of a soft final-state parton and to understand the correction that arise from the finite parton scattering kinematics, branching kinematics, and recoil of the constituents of the QCD medium is the main goal of this Letter.

The rest of this Letter is organized as follows: in section II we discuss the theoretical framework $\mathrm{SCET_G}$ for our calculation and demonstrate how the vacuum Altarelli-Parisi splitting kernels can be derived in Soft Collinear Effective Theory. The derivation of the full splitting kernels for in-medium jet production with final-state interactions is discussed in section III. We elucidate the relation to early soft gluon approximation results and provide analytic formulas for simplified kinematics and medium geometry scenarios. Numerical control over the newly-derived medium-induced splitting intensities is demonstrated in section IV. In this section we also quantify the effects of large-x corrections, finite kinematics, and medium recoil. A brief summary and outlook is presented in section V.

II. THEORETICAL FRAMEWORK

An effective theory, well-suited to describing the propagation of jets in the medium, has been recently developed in Ref. [40]. The Lagrangian of this EFT is given by the sum of the SCET Lagrangian [25–28] and a term that specifies the interactions of collinear partons in QCD

matter:

$$\begin{aligned}\mathcal{L}_{\mathrm{SCET_G}}(\xi_n, A_n, A_G) &= \mathcal{L}_{\mathrm{SCET}}(\xi_n, A_n) + \mathcal{L}_{\mathrm{G}}(\xi_n, A_n, A_G)\,,\\ \mathcal{L}_{\mathrm{G}}(\xi_n, A_n, A_G) &= \sum_{p,p'} \mathrm{e}^{-i(p-p')x}\Big(\bar{\xi}_{n,p'}\Gamma^{\mu,a}_{\mathrm{qqA_G}}\frac{\bar{\not{n}}}{2}\xi_{n,p}\\ &\quad -i\Gamma^{\mu\nu\lambda,abc}_{\mathrm{ggA_G}}\left(A^b_{n,p'}\right)_\nu\left(A^c_{n,p}\right)_\lambda\Big)\,A_{\mathrm{G}\,\mu,a}(x)\,.\end{aligned} \tag{1}$$

In Ref. [40] the vertexes $\Gamma^{\mu,a}_{\mathrm{qqA_G}}, \Gamma^{\mu\nu\lambda,abc}_{\mathrm{ggA_G}}$ have been derived for three types of gauge-fixing conditions: covariant, light-cone and hybrid gauges. In the first case we gauge-fix both the physical collinear gluons as well as the Glauber gluons in the covariant gauge. The second choice corresponds to gauge-fixing both fields using the light-cone gauge. The third choice, which appears to be the most convenient from the practical point of view, corresponds to a light-cone gauge for collinear gluons and a covariant gauge for the Glauber gluons. This is a legitimate choice from effective theory point of view, since we are allowed to gauge-fix separate gauge sectors independently. Another way of justifying this gauge choice is factorization between the splitting and the elastic scattering. In this hybrid case both the collinear Wilson line W and the transverse gauge link T [42–44] vanish. Gauge invariance of the physics results for the in-medium elastic scattering and radiative energy loss was demonstrated in [40], providing a cross-check on the approach and the newly-derived Feynman rules. It is interesting to note that the same effective theory $\mathrm{SCET_G}$ is relevant for describing the Drell-Yan process, as shown in Ref. [45].

We start from amplitudes for the parton splitting processes:

$$A_{q\to qg} = \langle q(p)g(k)|\,T\,\mathrm{e}^{iS}\,\bar{\chi}_n(x_0)\,|q(p_0)\rangle\,, \tag{2}$$
$$A_{g\to gg} = \langle g(p)g(k)|\,T\,\mathrm{e}^{iS}\,\mathcal{B}^{\lambda c}(x_0)\,|g(p_0)\rangle\,, \tag{3}$$
$$A_{g\to q\bar{q}} = \langle q(p)\bar{q}(k)|\,T\,\mathrm{e}^{iS}\,\mathcal{B}^{\lambda c}(x_0)\,|g(p_0)\rangle\,, \tag{4}$$
$$A_{q\to gq} = \langle g(p)q(k)|\,T\,\mathrm{e}^{iS}\,\bar{\chi}_n(x_0)\,|q(p_0)\rangle\,, \tag{5}$$

where $\chi, \mathcal{B}$ are collinear gauge invariant SCET fields [46, 47] and the momentum four-vectors, such as $p_0 = p + k$, are parametrized in the standard way, consistent with energy momentum conservation and the on-shell condition $p^2 = k^2 = 0$:

$$p_0 = \left[p_0^+, \frac{\mathbf{k}_\perp^2}{x(1-x)p_0^+}, \mathbf{0}_\perp\right], \tag{6}$$
$$p = \left[(1-x)p_0^+, \frac{\mathbf{k}_\perp^2}{(1-x)p_0^+}, -\mathbf{k}_\perp\right], \tag{7}$$
$$k = \left[xp_0^+, \frac{\mathbf{k}_\perp^2}{xp_0^+}, \mathbf{k}_\perp\right]. \tag{8}$$

We use square brackets to indicate the light-cone notation, which we define for arbitrary four-vector q in the following way: $q \equiv [q^+, q^-, \boldsymbol{q}_\perp] = [\bar{n}\cdot q, n\cdot q, \boldsymbol{q}_\perp]$ and $n^\mu = (1,0,0,1)\,, \bar{n}^\mu = (1,0,0,-1)$. The action in Eq. (2)-Eq. (5) is given by Lagrangian of $\mathrm{SCET_G}$:

$$S = i\int \mathrm{d}^4x\,\mathcal{L}_{\mathrm{SCET_G}}. \tag{9}$$

The Lagrangian of $\mathrm{SCET_G}$ [36, 40] is given in Eq. (1) and it evolves the created jet and describes the parton splitting processes and the interaction of the parton shower in the medium. The amplitude with $q\bar{q} \leftrightarrow \bar{q}q$ is not shown explicitly.

Restricting ourselves to the SCET Lagrangian without Glauber gluons, we first verify that at tree level we recover the Altarelli-Parisi splitting kernels [48], which have been originally calculated in full QCD:

$$\left(\frac{dN}{dx\,d^2\mathbf{k}_\perp}\right)_{q\to qg} = \frac{\alpha_s}{2\pi^2}C_F\frac{1+(1-x)^2}{x}\frac{1}{\mathbf{k}_\perp^2}, \tag{10}$$
$$\left(\frac{dN}{dx\,d^2\mathbf{k}_\perp}\right)_{g\to gg} = \frac{\alpha_s}{2\pi^2}2C_A\Big(\frac{1-x}{x}+\frac{x}{1-x} +x(1-x)\Big)\frac{1}{\mathbf{k}_\perp^2}, \tag{11}$$
$$\left(\frac{dN}{dx\,d^2\mathbf{k}_\perp}\right)_{g\to q\bar{q}} = \frac{\alpha_s}{2\pi^2}T_R\,\left(x^2+(1-x)^2\right)\frac{1}{\mathbf{k}_\perp^2}, \tag{12}$$
$$\left(\frac{dN}{dx\,d^2\mathbf{k}_\perp}\right)_{q\to gq} = \left(\frac{dN}{dx\,d^2\mathbf{k}_\perp}\right)_{q\to qg}(x\to 1-x). \tag{13}$$

We note that we are interested in real splitting processes away from the singular end points $x = 0$ and $x = 1$. In all expressions above the transverse momentum $\boldsymbol{k}_\perp$ and the lightcone momentum fraction $x = k^+/p_0^+ = k^+/(p^+ + k^+)$ are for the second final-state parton. The parent parton has no net transverse momentum and $\boldsymbol{k}_\perp = -\boldsymbol{p}_\perp$. Note that Eq. (10) and Eq. (13) are interchangeable under $x \to 1-x$, whereas Eq. (11) and Eq. (12) are symmetric under this substitution. The same symmetries hold for the medium-induced splittings that we derive in section III.

In this paper we use the following terminology: the double differential distribution $dN/dxd^2\mathbf{k}_\perp$ we call a splitting kernel, xdN/dx we call a splitting intensity and dN/dx we call a differential emitted parton number distribution. This terminology applies to both vacuum and medium-induced splittings. The $x-$dependent part of the vacuum splitting kernel we call a splitting function. Since the medium-induced kernel has a more complicated $\boldsymbol{k}_\perp, x$ correlation structure compared to the simple factorized form in Eq. (10) – Eq. (13) we avoid definition of a similar term in the medium.

III. MEDIUM-INDUCED PARTON SPLITTINGS

To describe the collisional and radiative processes for partons propagating in QCD matter, both single

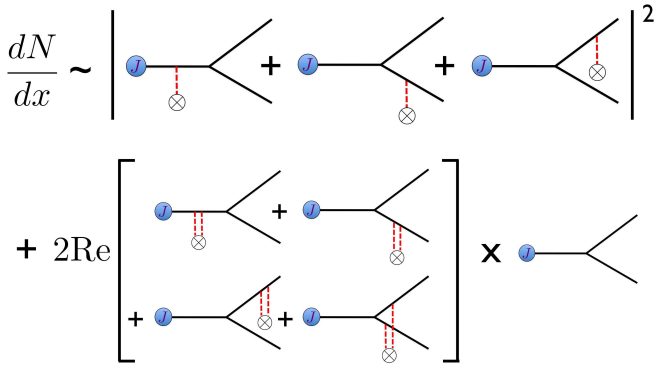

FIG. 1: Feynman diagrams contributing to medium-induced splittings at first order in opacity. Red lines corresponds to Glauber gluons. The kinematics and topology are common to all splitting processes: $q \to qg$, $g \to gg$, $g \to q\bar{q}$, $q \to gq$.

and double Glauber gluon exchanges between the jets and the constituents of the medium must be considered [40, 41, 50]. The calculation to first order in opacity, which takes into account the contribution from the splitting induced by the interactions along the trajectory of the parent parton and the dominant interference with the splitting induced by the large Q^2 process, is illustrated in figure 1. We do not specify the parent and daughter parton flavors since the topology and kinematics are the same for the splitting processes enumerated in Eqs. (10) - (13). Consequently, all results can be expressed in terms of universal transverse momentum vectors $\boldsymbol{A}_\perp, \boldsymbol{B}_\perp, \boldsymbol{C}_\perp, \boldsymbol{D}_\perp$ and interference phases $\Omega_1, ..., \Omega_5$, defined in [40]:

$$\boldsymbol{A}_\perp = \boldsymbol{k}_\perp,\ \boldsymbol{B}_\perp = \boldsymbol{k}_\perp + x\boldsymbol{q}_\perp,\ \boldsymbol{C}_\perp = \boldsymbol{k}_\perp - (1-x)\boldsymbol{q}_\perp,$$
$$\boldsymbol{D}_\perp = \boldsymbol{k}_\perp - \boldsymbol{q}_\perp, \tag{14}$$
$$\Omega_1 - \Omega_2 = \frac{\boldsymbol{B}_\perp^2}{p_0^+ x(1-x)},\ \Omega_1 - \Omega_3 = \frac{\boldsymbol{C}_\perp^2}{p_0^+ x(1-x)},$$
$$\Omega_2 - \Omega_3 = \frac{\boldsymbol{C}_\perp^2 - \boldsymbol{B}_\perp^2}{p_0^+ x(1-x)},\ \Omega_4 = \frac{\boldsymbol{A}_\perp^2}{p_0^+ x(1-x)},$$
$$\Omega_5 = \frac{\boldsymbol{A}_\perp^2 - \boldsymbol{D}_\perp^2}{p_0^+ x(1-x)}, \tag{15}$$

where $p_0^+ = p^+ + k^+$ and the parent parton has no net transverse momentum.

For completeness, we first present below the result for the $q \to qg$ splitting, calculated in [40] and shown to be gauge invariant:

$$\left(\frac{dN}{dx d^2\boldsymbol{k}_\perp}\right)_{q\to qg} = \frac{\alpha_s}{2\pi^2} C_F \frac{1+(1-x)^2}{x} \int \frac{d\Delta z}{\lambda_g(z)} \int d^2\mathbf{q}_\perp \frac{1}{\sigma_{el}} \frac{d\sigma_{el}^{\rm medium}}{d^2\mathbf{q}_\perp} \left[\frac{\boldsymbol{B}_\perp}{\boldsymbol{B}_\perp^2}\cdot\left(\frac{\boldsymbol{B}_\perp}{\boldsymbol{B}_\perp^2} - \frac{\boldsymbol{C}_\perp}{\boldsymbol{C}_\perp^2}\right)\right.$$
$$\times\left(1-\cos[(\Omega_1-\Omega_2)\Delta z]\right) + \frac{\boldsymbol{C}_\perp}{\boldsymbol{C}_\perp^2}\cdot\left(2\frac{\boldsymbol{C}_\perp}{\boldsymbol{C}_\perp^2} - \frac{\boldsymbol{A}_\perp}{\boldsymbol{A}_\perp^2} - \frac{\boldsymbol{B}_\perp}{\boldsymbol{B}_\perp^2}\right)\left(1-\cos[(\Omega_1-\Omega_3)\Delta z]\right)$$
$$+\frac{\boldsymbol{B}_\perp}{\boldsymbol{B}_\perp^2}\cdot\frac{\boldsymbol{C}_\perp}{\boldsymbol{C}_\perp^2}\left(1-\cos[(\Omega_2-\Omega_3)\Delta z]\right) + \frac{\boldsymbol{A}_\perp}{\boldsymbol{A}_\perp^2}\cdot\left(\frac{\boldsymbol{D}_\perp}{\boldsymbol{D}_\perp^2} - \frac{\boldsymbol{A}_\perp}{\boldsymbol{A}_\perp^2}\right)\left(1-\cos[\Omega_4\Delta z]\right)$$
$$\left.-\frac{\boldsymbol{A}_\perp}{\boldsymbol{A}_\perp^2}\cdot\frac{\boldsymbol{D}_\perp}{\boldsymbol{D}_\perp^2}\left(1-\cos[\Omega_5\Delta z]\right) + \frac{1}{N_c^2}\frac{\boldsymbol{B}_\perp}{\boldsymbol{B}_\perp^2}\cdot\left(\frac{\boldsymbol{A}_\perp}{\boldsymbol{A}_\perp^2} - \frac{\boldsymbol{B}_\perp}{\boldsymbol{B}_\perp^2}\right)\left(1-\cos[(\Omega_1-\Omega_2)\Delta z]\right)\right], \tag{16}$$

where $\lambda_g(z)$ is the scattering length of a gluon in the medium and $(1/\sigma_{el})\ d\sigma_{el}^{\rm medium}/d^2\mathbf{q}_\perp$ stands for normalized elastic scattering cross section of a parton in the medium. Even though this quantity varies when parton is a quark or a gluon, in the high energy limit, when the $t-$ channel dominates the elastic scattering, this normalized cross section does not change significantly.

Using the Feynman rules of SCET$_{\rm G}$ in the hybrid gauge and the Feynman diagrams exactly analogous to the case of $q \to qg$ splitting considered in [40] and shown in figure 1, we derive the remaining parton splittings in the medium. The calculations are non-trivial and facilitated by intermediate results in [40]. As discussed in section II, the medium-induced splitting for $q \to gq$ can be obtained from Eq. (16) with the substitution $x \to 1-x$. Here, we skip the explicit expression for brevity. The remaining two splittings from a parent gluon are as follows:

$$\left(\frac{dN}{dxd^2\boldsymbol{k}_\perp}\right)_{\left\{\begin{array}{l} g\to gg \\ g\to q\bar{q}\end{array}\right\}} = \left\{\begin{array}{c} \frac{\alpha_s}{2\pi^2}\,2C_A\left(\frac{x}{1-x}+\frac{1-x}{x}+x(1-x)\right) \\ \frac{\alpha_s}{2\pi^2}T_R\left(x^2+(1-x)^2\right)\end{array}\right\}\int d\Delta z\left\{\begin{array}{c}\frac{1}{\lambda_g(z)}\\ \frac{1}{\lambda_q(z)}\end{array}\right\}\int d^2\mathbf{q}_\perp\frac{1}{\sigma_{el}}\frac{d\sigma_{el}^{\rm medium}}{d^2\mathbf{q}_\perp}$$
$$\times\left[2\,\frac{\boldsymbol{B}_\perp}{\boldsymbol{B}_\perp^2}\cdot\left(\frac{\boldsymbol{B}_\perp}{\boldsymbol{B}_\perp^2}-\frac{\boldsymbol{A}_\perp}{\boldsymbol{A}_\perp^2}\right)\left(1-\cos[(\Omega_1-\Omega_2)\Delta z]\right)+2\,\frac{\boldsymbol{C}_\perp}{\boldsymbol{C}_\perp^2}\cdot\left(\frac{\boldsymbol{C}_\perp}{\boldsymbol{C}_\perp^2}-\frac{\boldsymbol{A}_\perp}{\boldsymbol{A}_\perp^2}\right)\left(1-\cos[(\Omega_1-\Omega_3)\Delta z]\right)\right.$$
$$+\left\{\begin{array}{c}-\frac{1}{2}\\ \frac{1}{N_c^2-1}\end{array}\right\}\left(2\frac{\boldsymbol{B}_\perp}{\boldsymbol{B}_\perp^2}\cdot\left(\frac{\boldsymbol{C}_\perp}{\boldsymbol{C}_\perp^2}-\frac{\boldsymbol{A}_\perp}{\boldsymbol{A}_\perp^2}\right)\left(1-\cos[(\Omega_1-\Omega_2)\Delta z]\right)\right.$$
$$+2\,\frac{\boldsymbol{C}_\perp}{\boldsymbol{C}_\perp^2}\cdot\left(\frac{\boldsymbol{B}_\perp}{\boldsymbol{B}_\perp^2}-\frac{\boldsymbol{A}_\perp}{\boldsymbol{A}_\perp^2}\right)\left(1-\cos[(\Omega_1-\Omega_3)\Delta z]\right)-2\,\frac{\boldsymbol{C}_\perp}{\boldsymbol{C}_\perp^2}\cdot\frac{\boldsymbol{B}_\perp}{\boldsymbol{B}_\perp^2}\left(1-\cos[(\Omega_2-\Omega_3)\Delta z]\right)$$
$$\left.\left.+2\,\frac{\boldsymbol{A}_\perp}{\boldsymbol{A}_\perp^2}\cdot\left(\frac{\boldsymbol{A}_\perp}{\boldsymbol{A}_\perp^2}-\frac{\boldsymbol{D}_\perp}{\boldsymbol{D}_\perp^2}\right)\left(1-\cos[\Omega_4\Delta z]\right)+2\,\frac{\boldsymbol{A}_\perp}{\boldsymbol{A}_\perp^2}\cdot\frac{\boldsymbol{D}_\perp}{\boldsymbol{D}_\perp^2}\left(1-\cos[\Omega_5\Delta z]\right)\right)\right], \tag{17}$$

where $\lambda_q(z)$ is the scattering length of a quark in the medium and same comment applies to the quantity $(1/\sigma_{el})\ d\sigma_{el}^{\rm medium}/d^2\mathbf{q}_\perp$ as after Eq. (16). Note that up to the overall vacuum-like splitting functions and color factors reflected both in the mean free paths (quark versus gluon) and the corrections relevant beyond the small-x approximation, the structure of the answers is very similar. The symmetry of $g\to gg, g\to q\bar{q}$ splitting kernels under $x\to 1-x$ is most easily verified explicitly by realizing that the parton scattering cross section in the medium is invariant under $\boldsymbol{q}_\perp\to-\boldsymbol{q}_\perp$.

The basic features of the medium-induced parton splitting kernels are:

- In QCD, for parent quark they factorize from the hard scattering cross section up to a standard integral convolution [40]. For parent gluons non-trivial spin correlation are present analogous to the vacuum case [49].

- They are proportional to their vacuum Altarelli-Parisi splitting functions [48].

- The in-medium splittings are gauge-invariant, as they should be, since the underlying jet production process itself is gauge-invariant [40].

- The splitting kernels depend on the properties of the QCD matter and vanish when the size or density of the medium vanish. The functions derived here are only valid for final-state interactions [41].

It is instructive to verify that in the small-x limit only two of the four medium-induced splitting intensities survive and this allows for the standard energy loss interpretation of jet quenching:

$$x\left(\frac{dN}{dx}\right)_{\left\{\begin{array}{l} q\to qg \\ g\to gg \\ g\to q\bar{q} \\ q\to gq\end{array}\right\}} = \frac{\alpha_s}{\pi^2}\left\{\begin{array}{c} C_F[1+\mathcal{O}(x)] \\ C_A[1+\mathcal{O}(x)] \\ T_R[0+\frac{x}{2}+\mathcal{O}(x^2)] \\ C_F[0+\frac{x}{2}+\mathcal{O}(x^2)]\end{array}\right\}$$
$$\times\int d\Delta z\left\{\begin{array}{c}\frac{1}{\lambda_g(z)}\\ \frac{1}{\lambda_g(z)}\\ \frac{1}{\lambda_q(z)}\\ \frac{1}{\lambda_q(z)}\end{array}\right\}\int d^2\mathbf{k}_\perp d^2\mathbf{q}_\perp\frac{1}{\sigma_{el}}\frac{d\sigma_{el}^{\rm medium}}{d^2\mathbf{q}_\perp}$$
$$\times\frac{2\boldsymbol{k}_\perp\cdot\boldsymbol{q}_\perp}{\boldsymbol{k}_\perp^2(\boldsymbol{k}_\perp-\boldsymbol{q}_\perp)^2}\left[1-\cos\frac{(\boldsymbol{k}_\perp-\boldsymbol{q}_\perp)^2}{xp_0^+}\Delta z\right]. \tag{18}$$

In this limit the interference structure for all medium-induced splitting intensities is the same. Furthermore, in the small-x limit the last two splittings are suppressed ($\mathcal{O}(x)$) relative to the first two. We keep the first correction for numerical comparison only. The color structure for the in-medium interactions also simplifies in this limit and is determined by the flavor of the small-x parton in the final state. Specifically, the first two in-medium splittings are proportional to $1/\lambda_g$ and the second two are proportional to $1/\lambda_q$. In deriving these results, we have used relation: $\lambda_q/\lambda_g = C_A/C_F$, which follows from the leading order perturbation theory approximation. As expected, in the small-x emission limit our results coincide exactly with the intensity derived (or neglected when the leading term is 0) in [50].

In section IV we will study numerically the in-medium splittings derived here with an emphasis on going beyond the traditional small-x approximation and on including medium recoil. The remaining part of the current section is devoted to deriving analytic formulas for the inclusive splitting intensity $x(dN/dx)$ under certain idealized assumptions. This will, in turn, allow us to obtain fully analytic formulas that can be used to benchmark the re-

alistic numerical calculation.

A useful starting point for integrating the splitting kernels analytically over the transverse momenta is the following master formula:

$$\int d^2\boldsymbol{k}_\perp d^2\boldsymbol{q}_\perp \frac{1}{\sigma_{el}}\frac{d\sigma_{el}}{d^2\mathbf{q}_\perp}\frac{2\boldsymbol{k}_\perp\cdot\boldsymbol{q}_\perp}{\boldsymbol{k}_\perp^2(\boldsymbol{k}_\perp-\boldsymbol{q}_\perp)^2} \times\left[1-\cos(\alpha(\boldsymbol{k}_\perp-\boldsymbol{q}_\perp)^2)\right]=f[\alpha\mu^2], \quad (19)$$

where a specific form for elastic cross section was assumed as explained below and shown in Eq. (21), and function $f[x]$ equals:

$$f[x] \;=\; 2\pi\Big[\gamma_{\rm E}+\ln(x)+\frac{\pi}{2}\sin(x)-\cos(x)\mathrm{Ci}(x) -\sin(x)\mathrm{Si}(x)\Big]. \quad (20)$$

Two assumptions are already made at this level. First, we took the limits of integration on $\boldsymbol{k}_\perp, \boldsymbol{q}_\perp$ to infinity. In reality, phase space cuts affect the cross section and we study this effect numerically in the next section. Second, we neglected the recoil effect in the medium. In that approximation the normalized cross section equals:

$$\frac{1}{\sigma_{el}}\frac{d\sigma_{el}}{d^2\mathbf{q}_\perp}=\frac{\mu^2}{\pi(\boldsymbol{q}_\perp^2+\mu^2)^2}. \quad (21)$$

The effects of finite medium recoil are also studied in the next section numerically. It turns out that using Eq. (19) it is possible to calculate $\boldsymbol{k}_\perp, \boldsymbol{q}_\perp$ integrals in all in-medium splittings Eq. (16)-Eq. (17). The result is rather compact and can be expressed in terms of the function $f[x]$ defined in Eq. (20):

$$x\left(\frac{dN}{dx}\right)^{\infty}_{q\to qg}=x\frac{\alpha_s}{2\pi^2}C_F\frac{1+(1-x)^2}{x}\int\frac{d\Delta z}{\lambda_g(z)}\frac{f[\beta]+f[\beta(1-x)^2]-\frac{1}{N_c^2}f[\beta x^2]}{2}, \quad (22)$$

$$x\left(\frac{dN}{dx}\right)^{\infty}_{g\to gg}=x\frac{\alpha_s}{2\pi^2}2C_A\left(\frac{x}{1-x}+\frac{1-x}{x}+x(1-x)\right)\int\frac{d\Delta z}{\lambda_g(z)}\frac{f[\beta x^2]+f[\beta(1-x)^2]+f[\beta]}{2}, \quad (23)$$

$$x\left(\frac{dN}{dx}\right)^{\infty}_{g\to q\bar{q}}=x\frac{\alpha_s}{2\pi^2}T_R\left(x^2+(1-x)^2\right)\int\frac{d\Delta z}{\lambda_q(z)}\left[\frac{N_c^2}{N_c^2-1}\left(f[\beta x^2]+f[\beta(1-x)^2]\right)-\frac{1}{N_c^2-1}f[\beta]\right], \quad (24)$$

$$x\left(\frac{dN}{dx}\right)^{\infty}_{q\to gq}=x\left(\frac{dN}{dx}\right)^{\infty}_{q\to qg}(x\to 1-x), \quad (25)$$

where the superscript ∞ stands for infinite limits of integrations for $\boldsymbol{k}_\perp, \boldsymbol{q}_\perp$, and:

$$\beta\equiv\frac{\mu^2\Delta z}{p_0^+x(1-x)}. \quad (26)$$

In order to perform the remaining Δz integral, one has to specify the geometry and an expansion scenario for the QCD medium that the partons traverse. Even the simplest realistic model of the medium, which includes the Glauber nuclear geometry and Bjorken expansion, requires numerical evaluation of the in-medium splitting kernels. One can validate the numerical simulation techniques by comparing the results to closed-form analytic formulas for uniform QCD matter, where the parton mean free paths λ_q, λ_g and trajectory length L are fixed. Thus, it is instructive to have analytical formulas for splitting intensity for uniform QCD matter. By assuming constant $\lambda_{q,g}$ as a function of Δz, and integrating expressions in Eq. (22)-Eq. (25) over $0<\Delta z<L$, we obtain the following differential splitting intensities:

$$x\left(\frac{dN}{dx}\right)^{\infty,\mathrm{static}}_{q\to qg}=x\frac{\alpha_s}{2\pi}C_F\frac{1+(1-x)^2}{x}\frac{L}{\lambda_g}\left(g[\gamma]+g[\gamma(1-x)^2]-\frac{1}{N_c^2}g[\gamma x^2]\right), \quad (27)$$

$$x\left(\frac{dN}{dx}\right)^{\infty,\mathrm{static}}_{g\to gg}=x\frac{\alpha_s}{2\pi}2C_A\left(\frac{x}{1-x}+\frac{1-x}{x}+x(1-x)\right)\frac{L}{\lambda_g}\left(g[\gamma x^2]+g[\gamma(1-x)^2]+g[\gamma]\right), \quad (28)$$

$$x\left(\frac{dN}{dx}\right)^{\infty,\mathrm{static}}_{g\to q\bar{q}}=x\frac{\alpha_s}{2\pi}T_R\left(x^2+(1-x)^2\right)\frac{L}{\lambda_q}\left[\frac{2N_c^2}{N_c^2-1}\left(g[\gamma x^2]+g[\gamma(1-x)^2]\right)-\frac{2}{N_c^2-1}g[\gamma]\right], \quad (29)$$

where the function g is given by:

$$w\,g[w] \;\equiv\; \frac{\pi}{2}(1-\cos(w))+(\gamma_{\rm E}-1)w+w\ln(w) +\mathrm{Si}(w)\cos(w)-\mathrm{Ci}(w)\sin(w), \quad (30)$$

and γ is defined as:

$$\gamma \;\equiv\; \frac{\mu^2 L}{p_0^+x(1-x)}. \quad (31)$$

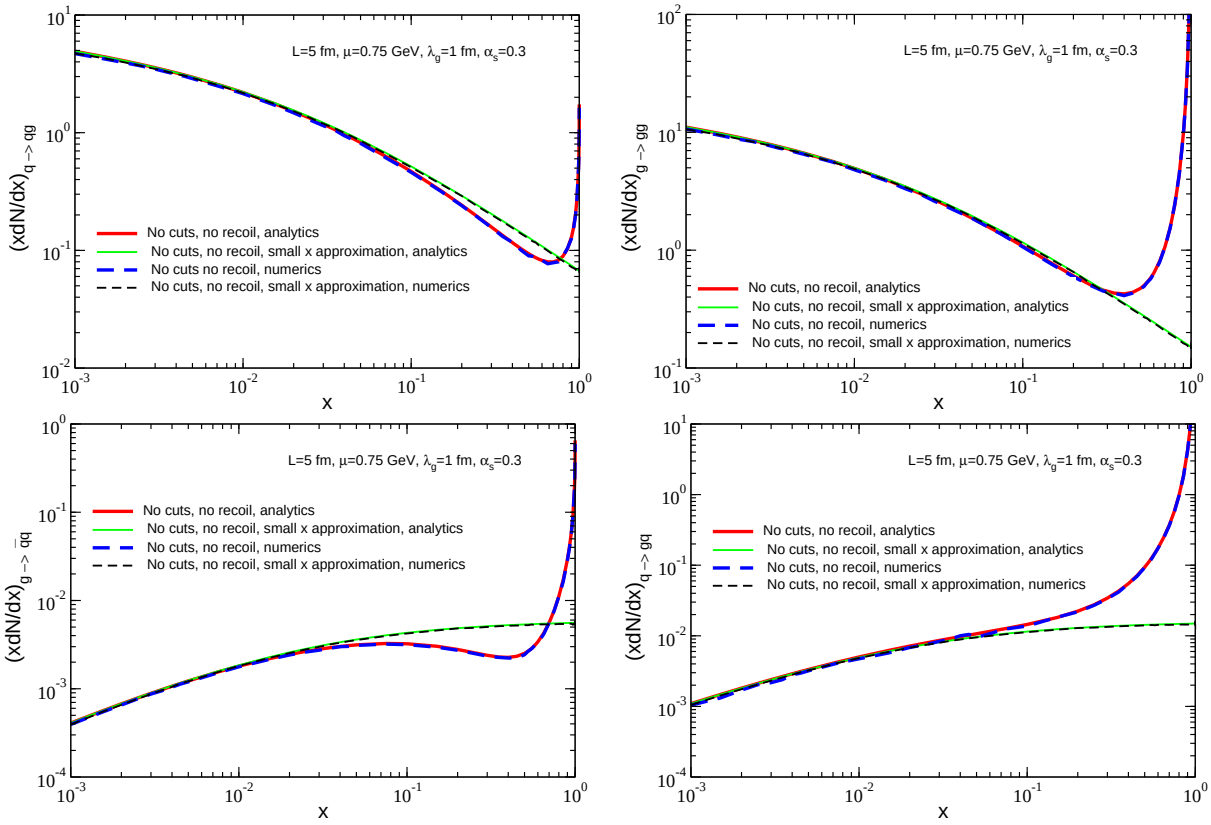

FIG. 2: The intensity spectrum $x(dN/dx)$ for infinite phase space cuts and neglecting nuclear recoil is shown as a function of the splitting parameter x. Comparison of the analytic formulas in Eq. (27)-Eq. (29) (solid lines) to a numerical integration method (dashed lines) are presented. We also illustrate the difference between the full in-medium splitting results and the small-x approximation on the example of a parton of initial energy $E_0 = 100$GeV. The medium parameters are set to: $\mu = 0.75$ GeV, $\lambda_g = 1$ fm, $L = 5$ fm for definiteness and the scattering length is independent of Δz.

The intensity spectrum for the last splitting $q \to gq$ can be obtained from substitution $x \to 1 - x$ in the $q \to qg$ splitting and is given in Eq. (25).

IV. NUMERICAL RESULTS

In this section we study the effects of kinematic cuts and recoil of the medium by evaluating dN/dx numerically. In so doing, we demonstrate control over the numerical evaluation, keeping in mind that future applications will require such approach to incorporate the finite kinematics, the spatially non-uniform and time-dependent density of the QCD matter, and the recoil of the in-medium partons. For each splitting we consider the full result given by Eq. (16) - Eq. (17) and compare it to the small-x limit presented in Eq. (18). In this paper we consider a medium of uniform density for simplicity and set the parameters of the simulation as follows: the typical inverse range of the parton scattering in the medium is $\mu = 0.75$ GeV, the size of the QCD medium is $L = 5$ fm, the gluon mean free path in matter is $\lambda_g = 1$ fm, and the parent parton energy is $E_0 = p_0^+/2 = 100$ GeV.

For infinite limits of the $\boldsymbol{k}_\perp, \boldsymbol{q}_\perp$ integrations, ignoring the medium recoil effects and assuming static QCD matter, we checked numerically our analytic formulas in Eq. (27) - Eq. (29). We found perfect agreement that validates the numerical integration methods and the analytic results. This can be seen from figure 2. Solid lines represents the analytic results of Eq. (27) - Eq. (29). Dashed lines represent numerical results. Our conclusions are valid for both the full in-medium splitting intensity $x(dN/dx)$ and its small-x limit. Note that for such comparison to be possible we have retained the subleading $\mathcal{O}(x)$ term for the $g \to q\bar{q}$ and $q \to gq$ processes. As expected, the deviation between the full in-medium splittings (red and blue lines) and their small-x approximation (green and black lines) is the largest as $x \to 1$. For intermediate $x \sim 0.5$ the deviation is on the order of a factor of 2 and changes sign.

In figure 3 we present the comparison of the splitting intensities without transverse momentum cuts and without parton recoil in the medium (solid red curve) to three different cut scenarios. In all three cases we use the same cut on $k_{\max} = \sqrt{Q^2 x(1-x)}$, which is unambiguous, and we choose $Q = E_0$. The three scenarios for the $\boldsymbol{q}_\perp$ cut are: *a*) the dashed green curve corresponds to

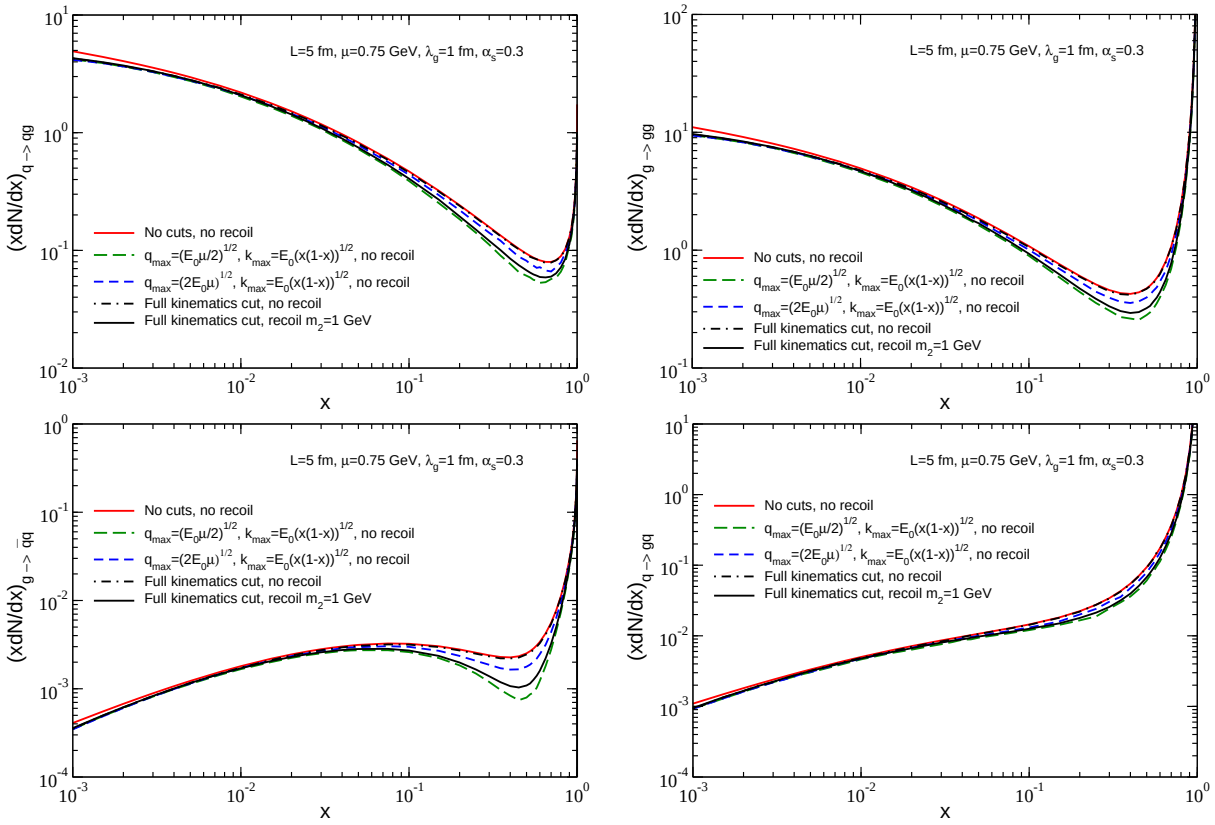

FIG. 3: Illustration of the effect of phase space cuts and medium recoil on the medium-induced parton splitting. The same QCD medium parameters and initial jet energy as in figure 2 are used.

$q_{\rm max} = \sqrt{\mu E_0/2}$, *b*) the dashed blue curve corresponds to $q_{\rm max} = \sqrt{2\mu E_0}$, *c*) the dot-dashed black curve corresponds to the exact phase space, given by $2 \to 2$ scattering available phase space. Finally, the solid black curve includes the recoil effect which is calculated by substituting the normalized cross section in Eq. (21) by the $2 \to 2$ t-channel differential cross section, which can be found in Eqs. (3.2-3.3) in Ref. [40]. From the definition of cut on $\boldsymbol{k}_\perp$, for small x we have $k_{\rm max} \sim Q\sqrt{x} \to 0$. From figure 3 one can see that for small x the cut on $\boldsymbol{k}_\perp$ is the only one that affects the splitting intensity, since all three types of cuts on $\boldsymbol{q}_\perp$ give practically identical results. As far as the intermediate x region is concerned, the cut on $\boldsymbol{k}_\perp$ does not play a significant role since from the definition $k_{\rm max}(x \sim 1/2) \sim Q/2$, thus the observable difference must be attributed to the cut on $\boldsymbol{q}_\perp$ for this region. The kinematic cut on $\boldsymbol{q}_\perp$, however, can lead to a factor of 2 variation of the in-medium parton splitting intensities at intermediate x. Note that for intermediate x the third cut on $\boldsymbol{q}_\perp$, which corresponds to full kinematics but retains the $1/\boldsymbol{q}_\perp^4$ dependence of the scattering cross section Eq. (21), agrees perfectly with the uncut solid red curve. In this case, cuts alone (in the sense of full kinematics) do not affect significantly the in-medium branching processes. We find that what affects the splitting intensity is the deviation between the exact scattering cross section from [40] and the approximate power-law form in Eq. (21). This is illustrated in figure 3 by the solid black curve that pushes the intensity of the medium-induced branching processes down when compared to the dot-dashed black curve. We finally note that if one wishes to simplify the calculation and use the approximate form Eq. (21) for in-medium parton scattering the most adequate transverse momentum cut would be $q_{\rm max} = \sqrt{\mu E_0}$. Finally, for $x \to 1$, we find that $k_{\rm max} \sim Q\sqrt{1-x} \to 0$, and all the splitting intensities with phase space cuts turn over at large enough x, which is not visible in figure 3 because we do not plot values of x very close to 1.

Numerically, all effects: finite x, phase space cuts, recoil effect are of the same order at high energies. In addition, we observe that parton recoil, similar to finite x corrections appears at intermediate x, while phase space cuts play role both for small x and intermediate x.

V. CONCLUSIONS

In this Letter we derived the medium-induced parton splittings for quarks and gluons produced in large Q^2 scattering processes that subsequently traverse a region of dense QCD matter and undergo final-state interactions using a recently constructed effective theory SCET$_{\rm G}$ [40]. Our results include both the contributions from the in-

medium parton scattering and their dominant interference with the vacuum-like branching processes [41, 50]. These formulas are valid for an arbitrary splitting parameter x and include all leading terms consistent with the power counting of $\mathrm{SCET_G}$ [40]. Our results for the $q \to qg$, $q \to gq$, $g \to gg$, $g \to q\bar{q}$, including Landau-Pomeranchuck-Migdal coherence and interference effects, are presented in Eq. (16)-Eq. (17) and are the main new findings reported in this Letter. We verified in Eq. (18) that in the small-x approximation our formulas simplify considerably and reduce to the soft gluon emission results of the Gyulassy-Levai-Vitev approach to inelastic parton interactions in dense QCD matter [41, 50]. In this case, to leading power in $1/x$, only two medium-induced splitting kernels survive that do not change the flavor of the leading parton and have a natural interpretation in terms of parton energy loss.

Neglecting the recoil of the partons in the QCD medium and ignoring the phase space cuts, we derived fully analytic formulas for the in-medium splitting intensity, given in Eq. (27)-Eq. (29). We see the main utility of these formulas as a convenient cross check for the numerical simulations, which we have demonstrated in this Letter. Our full results provide a basis for further improvements in the jet quenching phenomenology [10]-[15] by including the following effects: *a*) finite x corrections in the $q \to qg$ and $g \to gg$ splittings, consistent with the power counting of $\mathrm{SCET_G}$, *b*) new splittings for $g \to q\bar{q}$, $q \to gq$ from coherent final-state interactions, *c*) exact parton recoil kinematics and, *d*) exact phase space cuts. All of the above effects can be of the same order, as one can see from our numerical simulation results in section IV. This program of improving the theoretical accuracy of jet quenching simulations is especially interesting in light of recent RHIC and LHC heavy ion results [5]-[7], [17]-[23] and we plan to show first phenomenological applications in the near future.

Acknowledgments

This research is supported by the US Department of Energy, Office of Science, under Contract No. DE-AC52-06NA25396 and in part by the LDRD program at LANL and the JET topical collaboration.

[1] I. Arsene *et al.* [BRAHMS Collaboration], Nucl. Phys. A **757**, 1 (2005) [arXiv:nucl-ex/0410020].
[2] B. Back *et al.* [PHOBOS Collaboration], Nucl. Phys. A **757**, 28 (2005)
[3] J. Adams *et al.* [STAR Collaboration], Nucl. Phys. A **757**, 102 (2005) [arXiv:nucl-ex/0501009].
[4] K. Adcox *et al.* [PHENIX Collaboration], Nucl. Phys. A **757**, 184 (2005) [arXiv:nucl-ex/0410003].
[5] K. Aamodt *et al.* [ALICE Collaboration], Phys. Lett. B **696**, 30 (2011) [arXiv:1012.1004 [nucl-ex]].
[6] A. S. Yoon for the CMS collaboration, arXiv:1107.1862 [nucl-ex].
[7] A. Dainese for the ALICE Collaboration, arXiv:1106.4042 [nucl-ex].
[8] M. Gyulassy, I. Vitev, X. N. Wang and B. W. Zhang, arXiv:nucl-th/0302077.
[9] I. Vitev and B. W. Zhang, Phys. Rev. Lett. **104**, 132001 (2010) [arXiv:0910.1090 [hep-ph]].
[10] R. B. Neufeld, I. Vitev and B. W. Zhang, Phys. Rev. C **83**, 034902 (2011) [arXiv:1006.2389 [hep-ph]].
[11] I. P. Lokhtin, A. V. Belyaev and A. M. Snigirev, Eur. Phys. J. C **71**, 1650 (2011) [arXiv:1103.1853 [hep-ph]].
[12] G. Y. Qin and B. Muller, Phys. Rev. Lett. **106**, 162302 (2011) [arXiv:1012.5280 [hep-ph]].
[13] Y. He, I. Vitev and B. W. Zhang, arXiv:1105.2566 [hep-ph].
[14] R. B. Neufeld and I. Vitev, arXiv:1105.2067 [hep-ph].
[15] C. Mironov, M. Castro, P. Constantin, G. J. Kunde and R. Vogt, J. Phys. G **38**, 065002 (2011).
[16] R. B. Neufeld, arXiv:1108.6297 [nucl-th].
[17] S. Salur, Nucl. Phys. A **830**, 139C (2009) [arXiv:0907.4536 [nucl-ex]].
[18] M. Ploskon [STAR Collaboration], Nucl. Phys. A **830**, 255C (2009) [arXiv:0908.1799 [nucl-ex]].
[19] J. Jia, Nucl. Phys. A **855**, 92 (2011) [arXiv:1012.0858 [nucl-ex]].
[20] A. Angerami and A. Collaboration, arXiv:1108.5191 [nucl-ex].
[21] S. Chatrchyan *et al.* [CMS Collaboration], Phys. Rev. C **84**, 024906 (2011) [arXiv:1102.1957 [nucl-ex]].
[22] G. Aad *et al.* [Atlas Collaboration], Phys. Rev. Lett. **105**, 252303 (2010) [arXiv:1011.6182 [hep-ex]].
[23] S. Chatrchyan *et al.* [CMS Collaboration], Phys. Rev. Lett. **106**, 212301 (2011) [arXiv:1102.5435 [nucl-ex]].
[24] I. Vitev, S. Wicks and B. W. Zhang, JHEP **0811**, 093 (2008) [arXiv:0810.2807 [hep-ph]].
[25] C. W. Bauer, S. Fleming and M. E. Luke, Phys. Rev. D **63**, 014006 (2000) [arXiv:hep-ph/0005275].
[26] C. W. Bauer, S. Fleming, D. Pirjol and I. W. Stewart, Phys. Rev. D **63**, 114020 (2001) [arXiv:hep-ph/0011336].
[27] C. W. Bauer, D. Pirjol and I. W. Stewart, Phys. Rev. D **65**, 054022 (2002) [arXiv:hep-ph/0109045].
[28] C. W. Bauer and I. W. Stewart, Phys. Lett. B **516**, 134 (2001) [arXiv:hep-ph/0107001].
[29] S. Fleming, A. H. Hoang, S. Mantry and I. W. Stewart, Phys. Rev. D **77**, 114003 (2008) [arXiv:0711.2079 [hep-ph]].
[30] T. Becher and M. D. Schwartz, JHEP **0807**, 034 (2008) [arXiv:0803.0342 [hep-ph]].
[31] A. Hornig, C. Lee and G. Ovanesyan, JHEP **0905**, 122 (2009) [arXiv:0901.3780 [hep-ph]].
[32] R. Abbate, M. Fickinger, A. H. Hoang, V. Mateu and I. W. Stewart, Phys. Rev. D **83**, 074021 (2011) [arXiv:1006.3080 [hep-ph]].
[33] T. Becher, M. Neubert and G. Xu, JHEP **0807**, 030 (2008) [arXiv:0710.0680 [hep-ph]].
[34] I. W. Stewart, F. J. Tackmann and W. J. Waalewijn, Phys. Rev. D **81**, 094035 (2010) [arXiv:0910.0467 [hep-

ph]].
[35] T. Becher and M. D. Schwartz, JHEP **1002**, 040 (2010) [arXiv:0911.0681 [hep-ph]].
[36] A. Idilbi and A. Majumder, Phys. Rev. D **80**, 054022 (2009) [arXiv:0808.1087 [hep-ph]].
[37] F. D'Eramo, H. Liu and K. Rajagopal, arXiv:1006.1367 [hep-ph].
[38] M. Gyulassy, P. Levai and I. Vitev, Phys. Rev. D **66**, 014005 (2002) [arXiv:nucl-th/0201078].
[39] J. w. Qiu and I. Vitev, Phys. Lett. B **570**, 161 (2003) [arXiv:nucl-th/0306039].
[40] G. Ovanesyan and I. Vitev, JHEP **1106**, 080 (2011) [arXiv:1103.1074 [hep-ph]].
[41] I. Vitev, Phys. Rev. C **75**, 064906 (2007) [arXiv:hep-ph/0703002].
[42] X. d. Ji and F. Yuan, Phys. Lett. B **543**, 66 (2002) [arXiv:hep-ph/0206057].
[43] A. Idilbi and I. Scimemi, Phys. Lett. B **695**, 463 (2011) [arXiv:1009.2776 [hep-ph]].
[44] M. Garcia-Echevarria, A. Idilbi and I. Scimemi, Phys. Rev. D **84**, 011502 (2011) [arXiv:1104.0686 [hep-ph]].
[45] C. W. Bauer, B. O. Lange and G. Ovanesyan, JHEP **1107**, 077 (2011) [arXiv:1010.1027 [hep-ph]].
[46] C. M. Arnesen, J. Kundu and I. W. Stewart, Phys. Rev. D **72**, 114002 (2005) [arXiv:hep-ph/0508214].
[47] C. W. Bauer, O. Cata and G. Ovanesyan, arXiv:0809.1099 [hep-ph].
[48] G. Altarelli and G. Parisi, Nucl. Phys. B **126**, 298 (1977).
[49] S. Catani and M. Grazzini, Phys. Lett. B **446**, 143 (1999) [arXiv:hep-ph/9810389].
[50] M. Gyulassy, P. Levai and I. Vitev, Nucl. Phys. B **594**, 371 (2001) [arXiv:nucl-th/0006010].